

8 Centrifugal separation

The basic equations for most centrifugal modelling were introduced in Chapter 5. The liquid drag force was given in equation (5.4), under streamline flow, and the centrifugal field force was provided in equation (5.18). It is a simple matter to equate these to arrive at an analogue equation to the terminal settling velocity, equation (5.5), but with one significant difference

$$\frac{dr}{dt} = \frac{x^2(\rho_s - \rho)r\omega^2}{18\mu} \quad (8.1)$$

the distance with time differential is not constant. In a centrifugal field the particle moves radially, see Figure 8.1 and equation (5.18), and the radial position is part of the field force – hence the particle accelerates during its travel in the radial direction. Thus, to determine the particle position as a function of time integration is required.

It is well known that from a strict physical definition of forces on a particle, in circular motion, the *centripetal* force and not the centrifugal force should be considered. An unrestrained particle would leave its orbit tangentially if the centripetal force was suddenly removed. This is what happens with particles in cyclone separation from gases and this is discussed further in Chapter 14. However, this chapter is concerned with separation of particles in rotating flow within a viscous medium, usually water. The particle will not travel tangentially to one orbit, but to lots of orbits, giving the impression of radial movement outwards (provided the particle is denser than the surrounding continuous phase). Mathematically, we can use the well-known expressions, such as equations (5.18) and (8.1), to describe this travel.

As illustrated in Figure 8.1, the centrifugal acceleration is simply the product of the radial position (r) and the square of the angular velocity (ω). The SI units of angular velocity are s^{-1} , but calculated by converting from revs per minute (rpm) into radians per second – then ignoring the dimensionless radian term. In solid body rotation, such as a centrifuge, this is easily calculated from the rotational speed, usually provided in rpm. Thus, 1 rpm is $2\pi s^{-1}$ as an angular velocity. In free body rotation, such as the hydrocyclone, the angular velocity is calculated from the tangential velocity (u_θ) by

$$\omega = \frac{u_\theta}{r} \quad (8.2)$$

this is also illustrated on Figure 8.1. In the hydrocyclone the principle known as *the conservation of angular momentum* is used; in which knowledge of the tangential velocity at any radial position can be used to calculate the tangential velocity at another because

$$u_{\theta 1}r_1 = u_{\theta 2}r_2 = \text{constant} \quad (8.3)$$

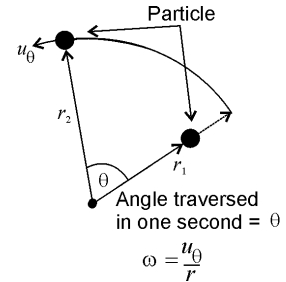


Fig. 8.1 Particle in rotation and definitions

Buoyancy

If a particle floats, rather than sinks, then it will move inwards in a centrifugal field. Particles denser than the fluid will move outwards. The centrifugal field acts like an enhanced gravitational field in equation (5.3) and it is usual to speak in terms of the equivalent 'g' force: i.e. centrifugal acceleration / 9.81 m s^{-2} .

or to take account of frictional losses within the hydrocyclone

$$u_{\theta 1} r_1^{n''} = u_{\theta 2} r_2^{n''} = \text{constant} \quad (8.4)$$

where n'' is an empirical constant, usually between 0.6 and 1.

In filtration within a centrifugal field the body force acts on the liquid, which can pass through the filter medium, or septum, similar to a washing machine or spin drier. The rotation acts in a similar way as increasing the pressure effecting the filtration and it is possible to deduce what this equivalent pressure difference is, using an equation analogous to that given by the static component of Bernoulli's equation (depth \times density \times acceleration)

$$\Delta P_{\text{CH}} = \rho \omega^2 (r_o^2 - r_L^2) / 2 \quad (8.5)$$

where r_o is the radius of the centrifuge and r_L is the inner liquid radial position and ΔP_{CH} is sometimes called the centrifugal head.

From all of the above, it should be apparent that modification of the equations discussed in Chapters 4 and 5, for an enhanced body force due to rotation is simply required.

8.1 Sedimenting centrifuges

The analogue continuous gravitational equipment design, to centrifuges, was covered in Section 5.4. Applying a similar logic to the critical trajectory model illustrated in Figure 5.6, the critical particle enters the centrifuge at radial position r_L and leaves at radial position r_o - assuming that the particle is denser than the liquid, see Figure 8.2. Equating the times taken for the particle to move radially and for it to progress axially provides the following expressions, based on equations (8.1) and (5.4)

$$t(\text{axial}) = \left[\frac{18\mu}{x^2(\rho_s - \rho)} \right] \frac{1}{\omega^2} \ln(r_o / r_L) \quad (8.6a)$$

$$t(\text{radial}) = \frac{\pi(r_o^2 - r_L^2)L}{2Q} \quad (8.6b)$$

where the equation (8.6b) is the volume of the machine divided by the volume flow rate; i.e. analogue to equation (5.4). Combining these equations and multiplying through by the acceleration due to gravity

$$\frac{\pi(r_o^2 - r_L^2)L}{2Q} = \left[\frac{18\mu}{x^2(\rho_s - \rho)g} \right] \frac{g \ln(r_o / r_L)}{\omega^2}$$

The term in the square brackets is the terminal settling velocity under gravity, equation (5.5), making this substitution and rearranging gives

$$\frac{Q}{U_t} = \frac{\pi(r_o^2 - r_L^2)L\omega^2}{g \ln(r_o / r_L)} \quad (8.7)$$

It is notable that the left hand side of equation (8.7) is identical to the left hand side of equation (5.28). Thus, equation (8.7) represents a centrifuge that has the same settling capacity as the plan area of a

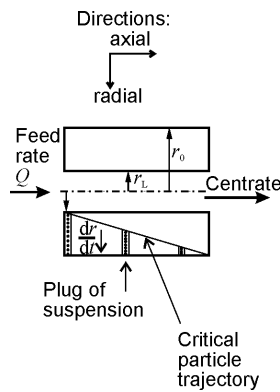


Fig. 8.2 Critical particle trajectory in a centrifuge

gravity settling basin. This is illustrated further as follows, the parameters that are defined by the process are called sigma-process

$$\Sigma_{\text{process}} = \frac{Q}{U_t} \tag{8.8}$$

i.e. for a given particle size there will be a certain flow rate (Q) at which all particles of this size are removed. If this flow rate is exceeded then particles of this size start to appear in the effluent. Thus, the process variables (size and flow rate) defines the sigma value. If the centrifuge is 100% efficient, the sigma process will be equal to the machine based parameters, called sigma-machine

$$\Sigma_{\text{machine}} = \frac{\pi(r_o^2 - r_L^2)L\omega^2}{g \ln(r_o / r_L)} \tag{8.9}$$

Both equations (8.8) and (8.9) have the SI units of area and both represent the theoretical plan area of a gravity settling basin that would perform the same separation duty on the solids. Introducing an efficiency factor (E_A) to take account of poor flow distribution within the machine and other factors reducing the separation capacity gives

$$\frac{Q}{U_t} = \frac{E_A \pi(r_o^2 - r_L^2)L\omega^2}{g \ln(r_o / r_L)} \tag{8.10}$$

It is worth noting that, under gravity, particles less than 2 μm in size might not settle because of molecular bombardment from the liquid and colloidal forces. However, in a centrifugal field the body force is much stronger and these particles have a greater chance of settling. Hence, a separation that might not be possible under gravity might be possible in a centrifuge. Obviously, a separation that is possible under gravity will be much quicker in a centrifuge, due to the enhanced g force. However, if there is little density difference between the particle and fluid the separation under gravity and in a sedimenting centrifuge will be slow, or impossible.

In a continuous sedimenting centrifuge there is always the problem of how to remove the deposited solids continuously and how to enhance the separation. Various designs are used including: scroll discharge decanter, time activated nozzle discharge disc stack and the continuous tubular centrifuge. These are illustrated in Figure 8.3. In the scroll discharge machine the Archimedean scroll rotates very slightly slower than the centrifuge, to convey the solids up the beach and out of the machine. The disc stack centrifuge provides a lot of parallel settling chambers, similar to the lamella separator in Figure 6.16. However, solids discharge is usually intermittent from this machine, limiting its application to low concentration slurries. In the tubular bowl centrifuge there are no internal structures, so it is possible to run the machine at very high rotational speeds, up to 30000 rpm. Continuous discharge relies upon flushing material out of the machine using displacement by incoming material and these devices are usually used on liquid/liquid separations or emulsions.

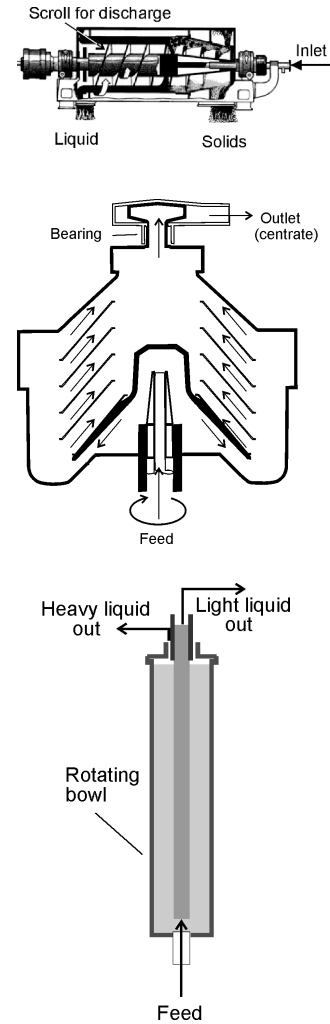


Fig. 8.3 Some sedimenting centrifuge designs

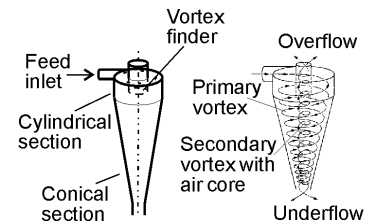
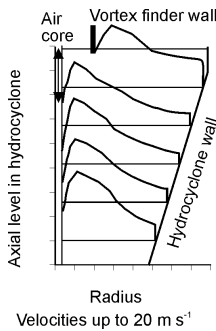


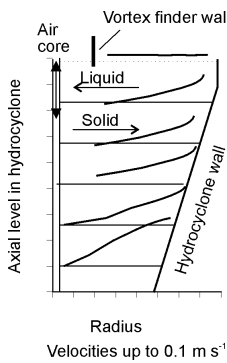
Fig. 8.4 The hydrocyclone and flow patterns inside

The machines with internal structures have slightly modified forms of the sigma expression to account for the differences in geometry. However, the sigma values are still related to the equivalent settling basin plan area.

tangential:



radial:



axial:

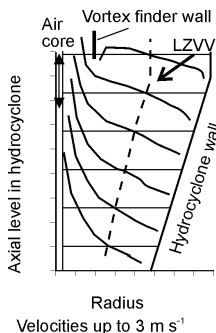


Fig. 8.5 Velocities within the hydrocyclone

8.2 Hydrocyclones

Figure 8.4 illustrates a hydrocyclone, including the flow patterns found within the device. The tangential inlet causes the fluid to rotate, rather than mechanically rotating the wall, hence these devices are described as having no moving parts. Of course, a pump or other prime mover for the suspension is required. The flow pattern within the hydrocyclone is complex and there are three velocities that need to be considered. The tangential velocity gives rise to particles subject to the centrifugal field force and is, therefore, critical to the operation of the hydrocyclone. Tangential velocities of the liquid, and solids, may be up to 20 m s^{-1} . The radial velocity is much lower, usually less than 0.1 m s^{-1} . However, within the device there is a net flow of liquid towards the centre and a net flow of solids away from it. Hence, it is important to distinguish between the radial liquid, or solid, flow. The third velocity is in the axial direction. This velocity has to be considered carefully because the hydrocyclone has two outlets, continuously splitting the feed in to two separate streams. The *overflow* contains a suspension that is more dilute than the feed and has a finer particle size distribution. By contrast, the *underflow* is a suspension more concentrated than the feed and has a coarser particle size distribution. Thus, the hydrocyclone acts as both a thickener (i.e. concentrates a suspension) and a classifier (i.e. selects particles of a specific size). The axial velocity must take material to the two outlets and the suspension near to the wall of the hydrocyclone flows axially to the underflow. The material near to the centre of the hydrocyclone flows axially to the overflow. Hence, there is axial flow downwards, and upwards, within the hydrocyclone as illustrated in Figure 8.5.

A further understanding of these axial flows can be obtained by considering the hydrocyclone primary and secondary vortices. The *primary vortex* spirals down towards the underflow taking the larger particles with it: these are centrifugally encouraged towards the wall of the hydrocyclone. However, the geometry of the hydrocyclone causes flow reversal towards the central axis of the device, giving rise to the *secondary vortex* that spirals upwards to the overflow. It is the finer particles that are caught within the secondary vortex. A *vortex finder* is used on the overflow to minimise *short circuiting* of solids from the feed directly to the overflow.

Referring to Figure 8.5, the argument can be made that because there is axial flow upwards into the overflow and downwards into underflow there must be a shear plane within the hydrocyclone where there is no net velocity in the axial direction. In fact, the shear plane is a surface, or locus, because the device is three dimensional;

hence, this has become known as the Locus of Zero Vertical Velocity (LZVV). However, it is a misnomer because the hydrocyclone could operate equally efficiently in any orientation and the term should really be locus of zero *axial* velocity. The concept of this LZVV is very important and it can be used to explain some of the observed behaviour in the hydrocyclone. Within the device it is possible to set up a force balance between the centrifugal force and the liquid drag force. The latter pulls the particles inwards, as liquid must flow inwards in order to enter the overflow. Hence, particles may adopt an orbit; where the drag force is balanced by the centrifugal force. Particles that orbit at a radial distance greater than the LZVV will be in the primary vortex and will tend to report to the underflow. Particles orbiting at radial distances less than the LZVV will be in the secondary vortex and will be carried into the overflow. Thus, the particle size that orbits at the LZVV will have no preference for the overflow or underflow; i.e. it will have an equal chance of entering either exit. This is defined as being the *cut size* (x_{50}) of the hydrocyclone, see Figure 8.7. Again, the term is misleading as it could be assumed that no particles bigger than the cut size enters the overflow; which is very significantly different from the true meaning of equal chance of entering either flows. For a particle to be radially stationary on the LZVV the force due to liquid drag inwards must be balanced by the particle centrifugal field force outwards, Figure 8.6

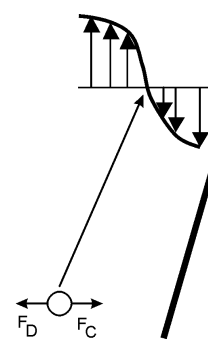


Fig. 8.6 Equilibrium orbit at the LZVV with liquid drag and centrifugal forces balanced

$$3\pi\mu x u_r = \frac{\pi x^3}{6} (\rho_s - \rho) r \omega^2$$

which can be rearranged to give

$$x_{50} = \sqrt{\frac{18\mu u_r}{(\rho_s - \rho)R\omega^2}} \tag{8.11}$$

where R is the radius of the LZVV. Hence, it is possible to predict the cut size of the hydrocyclone provided the terms on the RHS of equation (8.11) are known. This approach is known as the *equilibrium orbit theory*. There are three variables that must be deduced before the cut size can be estimated: the radial liquid velocity, the radial position of the LZVV and the angular velocity at the LZVV. The remaining physical constants should be straightforward to obtain.

The radial position of the LZVV is deduced by assuming that the LZVV is a shape that is identical to that of the overall hydrocyclone, but at a smaller radius, and that the volumetric flow split of overflow rate compared to feed rate is equal to the volume ratio within the hydrocyclone; i.e.

$$\frac{\text{volume inside LZVV}}{\text{volume inside hydrocyclone}} = \frac{\text{volume overflow rate}}{\text{volume feed rate}}$$

see Problem 8 for a worked example of this.

Once the radial position of the LZVV has been deduced it is possible to calculate the radial liquid velocity if it is assumed that the liquid flow entering the overflow is uniformly distributed over the

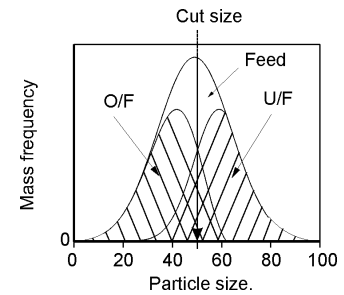


Fig. 8.7 Size distributions of feed, overflow and underflow showing the cut size. Note that this is an idealised plot assuming equal volume flow split between the underflow and overflow – hence the two outlet curves should equal the feed curve.

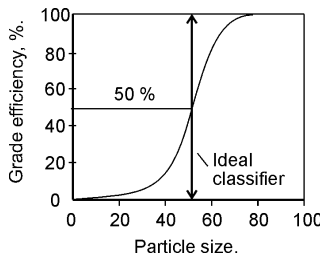


Fig. 8.8 Reduced grade efficiency curve and ideal classifier showing a vertical line at the cut size.

Grade efficiency

In particle classification it is usual to have a single feed stream and two outlet streams – one with particles finer than the other, and it is usual to define the grade efficiency as being the fraction by mass of particles reporting to the fine cut of the classifier. Grade efficiency in hydrocyclones is defined as fraction by mass entering the underflow, i.e. the coarser cut. It is also sometimes called the recovery curve. With the term grade efficiency care is always needed to determine if the definition is recovery to the fine, or coarse, fraction from the classifier.

entire surface of the LZVV. Hence, after calculating the equilibrium orbit radius (R) the surface area of the LZVV can be deduced from the equations of surface area of a cylinder and cone, see the Problems for these. The radial liquid velocity inwards is then the volume flow rate in the overflow divided by this surface area. The angular velocity at R is deduced using equations (8.2) and (8.3). Firstly, the tangential velocity at the inlet to the hydrocyclone is determined by dividing the feed rate by the cross-sectional area of the feed pipe. This gives the tangential velocity at the wall of the hydrocyclone, equation (8.3), or (8.4), can be used to convert this to tangential velocity at the LZVV and equation (8.2) is used to deduce the angular velocity at this point.

Experimental observations performed using glass and transparent plastic hydrocyclones have shown that there exists a *mantle* region within the hydrocyclone, in which there is little radial flow over the LZVV. The experimenters injected a pulse of dye into the hydrocyclone and it remained at the LZVV corresponding to the region where the hydrocyclone is cylindrical, but not the conical section; i.e. the dye did not accumulate in the conical section. Hence, in order to use equation (8.11) the liquid velocity inwards can be modified by neglecting the surface area of the cylindrical section of the LZVV; i.e. the overflow rate divided by the surface area of the conical section of the LZVV gives the liquid velocity corrected for no-flow over the mantle region.

Equation (8.11) can be used to deduce the cut size, but it does not provide any information on the proportion of particles finer than the cut size that will enter the underflow (other than the knowledge that this will be less than 50%), nor on the proportion of particles larger than the cut size that will enter the overflow. This information is provided in the *grade efficiency curve*, which is illustrated by Figures 8.7 and 8.8. The formal definition of grade efficiency (E_1) is given below

$$E_1 = \frac{\text{Mass flow in size grade in underflow (kg s}^{-1}\text{)}}{\text{Mass flow in size grade in feed (kg s}^{-1}\text{)}} \quad (8.12)$$

However, there is a problem with this simple definition of grade efficiency: if the feed was simply taken into a box and split into two separate outlets, with equal flows, the grade efficiency according to equation (8.12) would be 50%, but the system has not achieved any degree of particle classification (sorting by size). To overcome this shortcoming the *reduced grade efficiency* is used, which is the grade efficiency by equation (8.12) minus the volumetric flow split entering the underflow. The volumetric flow split is known as the recovery (R_f). In practice, using this definition for reduced grade efficiency will result in values approaching zero for small particle sizes, but at larger particle sizes the values will be 100% minus the recovery. Whereas the value at larger particle sizes should be 100%. Hence, a modified reduced grade efficiency is usually used, with the correct limits of zero at low particle size and 100% at high sizes

$$\text{Reduced grade efficiency} = E_2 = \frac{E_1 - R_f}{1 - R_f} \tag{8.13}$$

and a sharpness of separation can be deduced from

$$\text{Sharpness of separation} = \frac{x_{25\%}}{x_{75\%}} \tag{8.14}$$

A residence time model for hydrocyclones, similar to that derived for centrifuges before equation (8.7), provides the following result

$$\frac{x_{50}^2 (\rho_s - \rho)L\Delta P}{\mu\rho Q} = 3.5 \tag{8.15}$$

The derivation was first published by Rietema and his work was later extended by Svarovsky. Consideration of equation (8.15) leads to the conclusion that there should be an optimum design: minimising cut size and pressure drop and maximising flow rate. Equation (8.15) is useful as it relates cut size to pressure drop over the hydrocyclone.

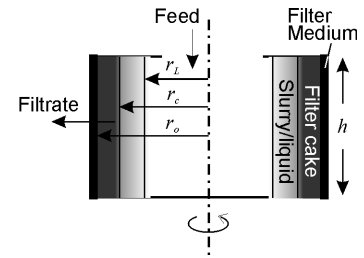


Fig. 8.9 Definition of terms within a filtering centrifuge

8.3 Filtering centrifuges

A schematic illustration of a filtering centrifuge is shown in Figure 8.9. As with sedimenting centrifuges, a major design consideration is the removal of solids in order to permit continuous operation of the industrial equipment. In filtering centrifuges, a more coherent solid structure is obtained due to the two forms of *dewatering* that apply: centrifugation and filtration. However, mechanical devices are still required to remove the cake in a semi-continuous manner. This can be achieved by the methods described in the box.

In most of the above filtering centrifuge types there is an identifiable cycle which is illustrated in the following table.

Table 8.1 Centrifuge full cycle

Function	Time (s)	Cycle time (%)
Accelerate 50 to 500 rpm	40	5
Load & filter at 500 rpm	277	32
Accelerate to 1050 rpm	90	10
Spin dry at 1050 rpm	119	14
Wash at 1050 rpm	10	1
Spin dry at 1050 rpm	236	27
Slow down to 50 rpm	90	10
Discharge at 50 rpm	15	2
Total cycle time	877	100%
Basket load per cycle of solids	140	kg
Productivity	575	kg h ⁻¹

Cake removal
 An oscillating plate that pushes the cake out of the machine in a *pusher centrifuge*, a knife that periodically enters the cake and scrapes it away in a *peeler centrifuge* and a rotating filter bag that is periodically pulled inside out; thus discharging its contents in the *inverting bag centrifuge*, the latter is a popular centrifuge type within the pharmaceutical industry. It is also possible to stop a centrifuge and manually dig the cake away.

The operations in italics in Table 8.1 are considered in the rest of this chapter, starting with the modification of the filtration theory already

Equipment

See:
www.midlandit.co.uk/particletechnology
 for links to equipment suppliers with pictures of the equipment described here.

covered in Chapter 4, to account for its application in a centrifugal field and filtering on the inside of a cylindrical surface.

It is possible to combine the basic filtration equations (4.7) and (4.10) and rearrange to give

$$\Delta P = \mu \left(\frac{\alpha c V}{A} + R_m \right) \frac{Q}{A} \tag{8.16}$$

However, when filtering on the inside of a cylinder the effective filtering area will be continually decreasing because of the shrinking of the radius on which the new cake forms. Hence, a consideration of the two areas contributing towards the equations (4.7) and (4.10), provides the alternative form to equation (8.16)

$$\Delta P = \mu \left(\frac{\alpha c V}{A^2} + \frac{R_m}{A_o} \right) Q \tag{8.17}$$

where A_o is the area before any solids deposition occurs and is

$$A_o = 2\pi r_o h \tag{8.18}$$

See Figure 8.9 for an illustration of these terms. Integration of equation (8.17), under constant pressure conditions, provides

$$Q = \frac{\Delta P}{\left[\frac{\mu \alpha c V}{A_{lm} A_{av}} + \frac{\mu R_m}{A_o} \right]} \tag{8.19}$$

where A_{lm} and A_{av} are the log-mean and average areas respectively. They can be calculated from

$$A_{lm} = \frac{2\pi h (r_o - r_c)}{\ln(r_o / r_c)} \tag{8.21}$$

$$A_{av} = \frac{2\pi h (r_o + r_c)}{2} \tag{8.22}$$

For filtering centrifuges the constant pressure, to be used in equation (8.19), can be calculated by equation (8.5). For data analysis, equation (8.19) can be rearranged into the form

$$\frac{t}{V} = \left(\frac{\mu \alpha c}{A_{lm} A_{av} \Delta P} \right) \frac{V}{2} + \frac{\mu R_m}{A_o \Delta P} \tag{8.23}$$

a similar relation to equation (4.19) which was used for constant pressure cake filtration analysis and illustrated in Figure 4.10. Equation (8.23) can be used for data analysis provided that the areas do not change significantly; this is true at the start of the filtration. Hence, under these conditions, a plot of t/V against V will be a straight line that can be used to deduce the filter cake specific resistance from the gradient and the cloth resistance from the intercept. Under these conditions A_o may need to be used for the log mean and average areas.

More detailed information on the areas can be obtained by conducting a material balance on the solids inside a batch centrifuge. Imagine a batch centrifugation has resulted in two products: a filtrate of volume V and a cake of volume hA . The balance provides:

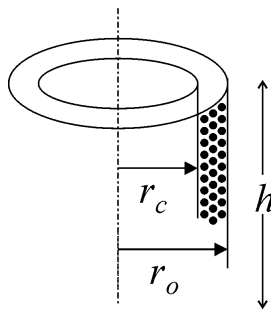


Fig. 8.10 Filtration on the inside of a cylinder – terms used in material balance

total volume slurry in the centrifuge was $(V+hA)$ m^3
 volume of solids at the start is $C_f(V+hA)$ m^3
 volume solids filtered and in cake is ChA m^3
 where C is the cake concentration and C_f the feed slurry concentration of solids, both by volume fraction. Hence, the mass balance on the solids gives

$$ChA = C_f(V + hA) \quad \text{which rearranges to} \quad hA = \frac{C_f}{C - C_f}V$$

and, see Figure 8.10, from the geometry the cake volume is

$$hA = h\pi(r_o^2 - r_c^2)$$

Hence, combining these equations and rearranging gives

$$r_c = \left(r_o^2 - \frac{C_f}{C - C_f} \frac{V}{\pi h} \right)^{1/2} \quad (8.24)$$

Equation (8.24) provides the cake radius as a function of filtrate volume, which can be used in equations (8.21) and (8.22) to give the filtering areas. This enables a more detailed analysis of the filtration data than that described under equation (8.23) and it can be used as part of the simulation, or modelling, of centrifugal filtration as described in Figure 8.11. Combining equations (8.19) to (8.22) and (8.5) for total pressure, noting that c is the dry cake mass per unit volume of filtrate, but forming inside a cylinder between r_o and r_c , i.e.

$$c = \frac{C(r_o - r_c)A_{av}\rho_s}{V} \quad (8.25)$$

provides the following simulation equation which is valid for filtration and for cake washing

$$Q = \frac{\rho_m \omega^2 (r_o^2 - r_L^2) / 2}{\left[\frac{\mu \alpha C \rho_s}{2\pi h} \ln\left(\frac{r_o}{r_c}\right) + \frac{\mu R_m}{2\pi r_o h} \right]} \quad (8.26)$$

where C is the cake concentration by volume fraction and ρ_m is the mean suspension density, see equation (6.12). During cake washing, the cake radius (r_c) will remain constant and the mean suspension density will be the density of the washing liquid, not including any solids. In many instances the liquid radius (r_L) is also a constant as the feed is controlled by an overflow weir.

8.4 Washing and dewatering

After filtration the cake will contain pores between the solids with retained solution present. In many cases, e.g. in some pharmaceutical formulations, it is not desirable to leave solutes from the initial reaction present in the final solid product. Hence, fresh solvent is used to wash the solutes from the cake, or at least to reduce their concentration to a low value. After washing to remove the solutes the

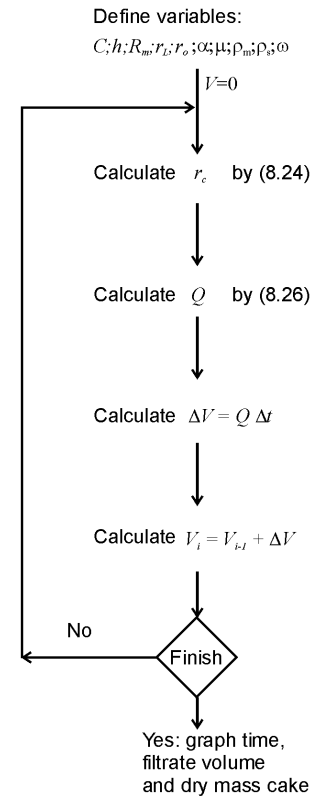


Fig. 8.11 Centrifugal filtration modelling as could be applied within a computer spreadsheet N.B. R_m must be finite to start solution off, its effect can be minimised by reducing Δt and comparing results as $R_m \rightarrow 0$

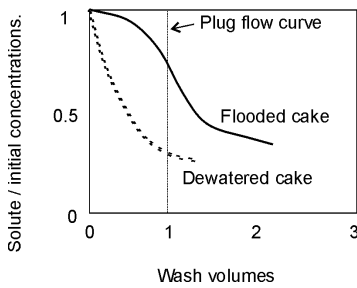


Fig. 8.12 Comparison of washing performance with dewatered and flooded cakes

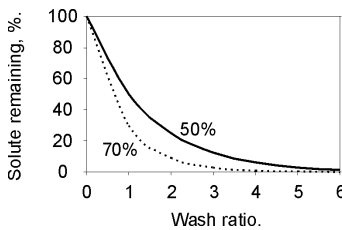


Fig. 8.13 Example washing performance at 50 and 70% efficiencies as provided by equation (8.28)

cake is often *dewatered* to reduce the amount of retained solvent in the pores between the solids forming the cake. The term dewatered is generally used regardless of whether the solvent is water, or otherwise. As the cake radius remains constant during washing, it is possible to integrate equation (8.26) directly for the time taken to wash the cake

$$t = \frac{\mu}{2\pi h \rho \omega^2 (r_o^2 - r_L^2) / 2} \left[\alpha C \rho_s \ln \left(\frac{r_o}{r_c} \right) + \frac{R_m}{r_o} \right] V_w \quad (8.27)$$

where V_w is the volume of wash water passed in the time t . The values to use in equations (8.26) and (8.27) for specific resistance and cake concentration could be obtained from conventional cake filtration tests and empirical relations such as equations (4.15) and (4.16), where cake forming pressure is obtained from equation (8.5).

Prior to washing, and as indicated in Table 8.1, it is usual to dewater the cake slightly. This will reduce the amount of solution that needs to be displaced from the cake and helps to reduce any inhomogeneity within the filter cake. Figure 8.12 compares the performance of cake washing with, and without, a dewatering stage before washing. The effectiveness of washing is usually judged by comparing the solute concentration in the filtrate with the value of solute in the solution. The *wash ratio* is the volume of wash liquid divided by the volume of the pores within the filter cake. Hence, under plug flow conditions, a wash volume of 1 would give a solute concentration of zero in the filtrate. In filter cakes the flow conditions can never be adequately described by plug flow, but a dewatered cake helps to reduce the volume of wash water required to obtain a given residual solute concentration.

For high removal of solute from the cake it may be necessary to *reslurry wash* the cake; i.e. take the dewatered filter cake and form another well dispersed slurry with it, then filter again. This is because cake washing on any filter is a mixture of displacement and diffusional flow of the solute and the latter process is very slow. The mass fraction of solute remaining in the washed cake (W_s) can be related to the wash ratio (W_R) and the washing efficiency (E_w) by the following equation

$$W_s = \left(1 - \frac{E_w}{100} \right)^{W_R} \quad (8.28)$$

Typical washing efficiencies are between 40 and 80%. An example wash ratio curve is illustrated in Figure 8.13.

After washing it is common to spin the cake as dry as possible, before discharge. There are two aspects to consider in this part of the dewatering process: the equilibrium residual moisture and the kinetic approach to that equilibrium. In the former case, for a given degree of force removing liquid from a cake (provided by a centrifugal field in this case) there will be a given amount of residual moisture retained by the capillary pressure force. This force is considered further in

Chapter 13. A finite time is required for the cake to drain, hence the rate of approach to the equilibrium saturation level of the filter cake is also important. The equilibrium saturation is known as the *irreducible saturation* and saturation is usually reported in terms of a ratio based on the initial value: i.e. after cake formation a fully saturated cake has a value of 1, but during dewatering the relative saturation approaches the irreducible saturation if sufficient time is allowed. This ratio of saturation values is known as the *relative saturation*. There are two well-known models for saturation modelling, one developed by Wakeman and based on particle properties and another based on the work of Zeitsch, which is based on a Boltzman distribution of pore diameters. However, in application the Zeitsch model applies the data obtained from the filtration stage and will be discussed further here.

The relation between filter cake permeability and cake specific resistance was provided in equation (4.12); permeability is used in Zeitsch's dimensionless Drainage (D_N) number

$$D_N = \frac{kr_o 2\omega^4 \rho^2 (r_o - r_c)^2}{(1-C)\sigma^2 \cos^2 \theta} \quad (8.29)$$

where σ is the surface tension and θ is the contact angle of the liquid on the solid. Zeitsch deduced the irreducible saturation (S_∞) to be

$$S_\infty = 1 - \exp\left(\frac{-1}{D_N}\right) + \frac{\sqrt{\pi D_N}}{2D_N} \left[1 - \operatorname{erf}\left(\frac{1}{\sqrt{D_N}}\right) \right] \quad (8.30)$$

The error function (erf) is built in to most modern spreadsheets, hence evaluation of operating parameters, such as rotational speed, by equations (8.29) and (8.30) on a spreadsheet is straightforward.

For a kinetic evaluation of drainage, Zeitsch defined a drainage rate constant (ϕ), which has the SI units of s^{-1} , as

$$\phi = \frac{\sigma^2 \cos^2 \theta}{2\mu(r_o - r_c)^3 \rho r_o \omega^2} \quad (8.31)$$

and, for convenience, it is possible to combine the drainage rate constant and drainage number into a single dimensionless term (B)

$$B = \frac{1}{D_N} + \phi t \quad (8.32)$$

where t is the time during drainage. According to the Zeitsch model, the relative saturation with respect to time is

$$S_t = S_\infty + \frac{1}{D_N^2 B} \left[\frac{1}{B} \exp(-B) - \frac{[1 - \operatorname{erf}(\sqrt{B})] \sqrt{\pi}}{2\sqrt{B}} \right] \quad (8.33)$$

Figure 8.14 provides an illustration of the above theory used to compare rotational speeds on relative saturation and drainage times.

On Figure 8.14, it is noticeable that there is little saturation reduction by spinning at 1400 rpm; the equilibrium value (irreducible

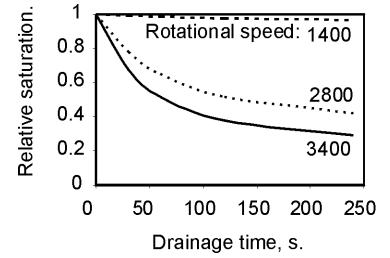


Fig. 8.14 Comparison of rotation speeds and resulting drainage curves.

Operating data:

filter diameter	0.3 m
solvent density	980 kg m ⁻³
solids density	1400 kg m ⁻³
solvent viscosity	0.001 Pa s
cake concn.	0.3 v/v
specific resistance	6x10 ¹⁰ m kg ⁻¹
rotational speed	3400 rpm
surface tension	0.07 N m ⁻¹
contact angle	10 Degrees
cake thickness	50 mm

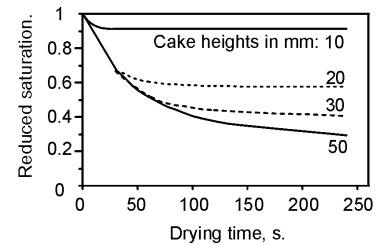


Fig. 8.15 Effect of cake thickness on saturation at a rotational speed of 3400 rpm – all other variables are as given below Figure 8.14

saturation) is 96%. At 3400 rpm the irreducible saturation is 24%. Hence, the beneficial effect of dewatering at higher rotational speeds is obvious. However, a relatively slow filtration rotational speed may be required to reduce the tendency for particles to penetrate the filter cloth. If this occurs the medium resistance term will increase and the cloth may even *blind*. Thus, gentle filtration conditions are often employed during the start of any filtration, building up to more severe dewatering conditions as time progresses. The data on Figure 8.14 demonstrates that there is a threshold pressure that needs to be overcome before significant dewatering occurs. The data on Figure 8.15 shows that dewatering is favoured by thicker cakes rather than thin ones. This is evident from a consideration of equations (8.29) and (8.30): the higher the drainage number the greater the dewatering will be. The rotational velocity has a significant effect on the dewatering as it is raised to the power 4 in the expression and the cake thickness ($r_o - r_c$) is raised to the power 2. Clearly, the benefit from increasing the cake thickness, on the reduction in cake moisture, becomes less significant at higher depths. Also, productivity calculations often suggest that thin cakes provide greatest throughputs; so, it is likely that there is an optimum cake thickness for any operation and that it is a balance between filtration, washing and dewatering requirements. The analysis provided by the above equations can be used to deduce that optimum cake height and, therefore, optimum throughput provided the numerical input variables are known, or can be measured.

8.5 Summary

A centrifugal field force can be used to speed up sedimentation and filtration. A sedimenting centrifuge, or hydrocyclone, may be used instead of gravity settlement and a filtering centrifuge enhances the rate at which liquid passes through the filter cake and cloth. In practice, in filtering centrifuges centrifugal sedimentation should be expected as well as filtration. The models of gravity sedimentation and pressure filtration were adapted to a centrifugal field force in this chapter.

8.6 Problems

1.

i). The equation for the rate at which a particle will settle in a *gravitational* field, neglecting the acceleration of the particle, is $U_t = \dots$

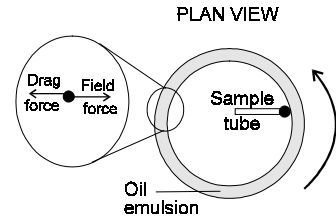
$$\text{a: } U_t = \frac{x^3(\rho_s - \rho)g}{18\mu} \quad \text{b: } U_t = \frac{x^2(\rho_s - \rho)g}{9\mu} \quad \text{c: } U_t = \frac{x^2(\rho_s - \rho)g}{18\mu}$$

ii). The equation for the rate at which a particle will move in a *centrifugal* field, neglecting the acceleration of the particle, is $dr/dt = \dots$

$$\text{a: } \frac{dr}{dt} = \frac{x^2(\rho_s - \rho)r\omega^2}{18\mu} \quad \text{b: } \frac{dr}{dt} = \frac{x^3(\rho_s - \rho)r\omega^2}{18\mu} \quad \text{c: } \frac{dr}{dt} = \frac{x^2(\rho_s - \rho)g}{18\mu}$$

iii). Why is the rate of motion radially in a centrifugal field not a constant, unlike settling under gravity?

iv). The diagram on the right illustrates a homogeneous oil emulsion contained in a circular channel rotating at 1000 rpm. The diameter of the outer circle is 30 cm, and the distance between the walls, i.e. the channel width is 2.5 cm. The angular velocity of the channel is (s^{-1}):
 a: 1000 b: 6280 c: 105 d: 3140



v). If the oil is less dense than the surrounding water an oil droplet will travel inwards on the application of a centrifugal field force, just as oil floats in a gravitational field. In the integration of the centrifugal rate expression with respect to time and radial distance, the upper or top limit of the integration of radial position is (cm):
 a: 30 b: 12.5 c: 15 d: 27.5

vi). The oil and water densities are 800 and 1000 $kg\ m^{-3}$, respectively and the viscosity of water is 0.001 Pa s, the time taken (neglecting acceleration) before a sample of emulsion withdrawn at the inner radius contains no particles bigger than 10 μm in diameter is (s):
 a: 15 b: 2290 c: -15 d: 150

2. In a continuous tube type centrifuge $5.4\ m^3\ min^{-1}$ of an aqueous suspension is being processed and all the particles of diameter 10 μm or more are being removed. The solid and liquid specific gravities are 2.8 and 1.0 respectively, and the liquid viscosity is 10^{-3} Pa s.

- i). The volume flow rate was ($m^3\ s^{-1}$):
 a: 0.0015 b: 0.09 c: 324 d: 5.4
- ii). Stokes' settling velocity of the 10 μm particle was ($m\ s^{-1}$):
 a: 9.8×10^{-6} b: 9.8×10^{-7} c: 1.5×10^{-4} d: 9.8×10^{-5}
- iii). The particle Reynolds number was:
 a: 2.7×10^{-3} b: 275 c: 9.8×10^{-5} d: 9.8×10^{-4}
- iv). The *sigma process* value was (m^2):
 a: 920 b: 150 c: 9200 d: 590

3. The machine used in the above question had a length and diameter of 1.5 and 0.75 m respectively. The pool depth (i.e. $r_o - r_L$) was 0.1 m, and the operating speed was 1800 rpm.

- i). The rotational speed was (s^{-1}):
 a: 190 b: 380 c: 11000 d: 94
- ii). The volume of the centrifuge pool ONLY was (m^3):
 a: 0.31 b: 0.20 c: 0.62 d: 0.05
- iii). The 'sigma machine' value was (m^2):
 a: 19 b: 840 c: 3600 d: 2200
- iv). Compare the two sigmas for the efficiency of the machine (%):
 a: 26 b: 4.3 c: 110 d: 30

Questions 2 and 5

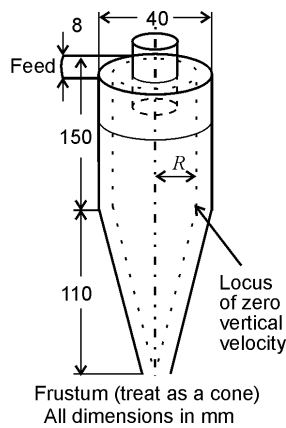
Consider the axial and radial flow in a tube centrifuge. If the start radius is, in fact, the inner diameter of the centrifuge, i.e. between r_L and the central axis there is only air, and we consider a critical particle trajectory we can derive the following equations

$$\Sigma_{PROCESS} = \frac{Q}{U_t}$$

where U_t is the terminal settling velocity of the critical particle under consideration. This is the area of a settling basin that would perform the same duty under the given flow rate. The theoretical capacity of the centrifuge is

$$\Sigma_{MACHINE} = \dots \frac{\pi(r_o^2 - r_L^2)L\omega^2}{g \ln(r_o / r_L)}$$

90 Centrifugal separation



The equilibrium orbit (R) of a particle at the locus of zero vertical velocity is given by

$$R = \frac{x^2(\rho_s - \rho) V_i^2}{18\mu U}$$

where V_i is the tangential velocity of the liquid in the hydrocyclone at the equilibrium orbit position and U is the inward radial velocity of the liquid. The principle of the conservation of angular momentum gives

$$V_i r_i = \text{constant}$$

and the surface area and volume of a cone are

$$\pi r l \quad \frac{\pi r^2 l}{3}$$

where l is height or length.

$$\frac{x^2(\rho_s - \rho)L\Delta P}{\mu\rho Q} = 3.5$$

4. The sigma values of four machines labelled a, b, c and d are 200, 400, 600 and 1200 m^2 , respectively. Assuming they cost the same, which machine would you recommend?

5.

i). Derive an expression for the volume fraction of a centrifuge, based on an imaginary *start radius* that exists between r_s and r_o (i.e. $p=$).

ii). Using r_s instead of r_L and equating the two sigma terms (see box above), derive an expression for r_s .

iii). Combine the answers to parts (i) and (ii) to give an expression for the proportion of particles removed as a function of flow and material properties, i.e. p or the grade efficiency= \dots

8. The feed and overflow rates of the hydrocyclone illustrated are 36 and 23 litres per minute, the liquid viscosity is 0.0015 Pa s, the solid and liquid densities are 2000 and 1000 kg m^{-3} , respectively. These questions determine the separation size for the hydrocyclone using equilibrium orbit theory.

i). If R_o is the internal radius of the hydrocyclone, the fractional volume inside the locus of zero vertical velocity is:

a: $(R/R_o)^3$ b: $(R/R_o)^2$ c: πR^2 d: lR^2/lR_o^2

ii). By assuming that the fractional volume inside the locus of zero vertical velocity is equal to the proportion of the feed flow going into the overflow (O/F), the equilibrium radius was (m):

a: 0.0052 b: 0.016 c: 0.032 d: 0.0080

iii). By considering the locus of zero vertical velocity as a surface over which the flow entering the O/F is uniformly distributed the liquid velocity over the LZVV was (m s^{-1}):

a: 0.025 b: 0.057 c: 0.0186 d: 0.069

iv). The inlet velocity, hence tangential velocity at R_o , was (m s^{-1}):

a: 5.97 b: 11.9 c: 7.32 d: 3.0

v). Using the principle of the conservation of angular momentum, and assuming that all the inlet flow occurs at R_o , the tangential velocity at the equilibrium orbit radius was (m s^{-1}):

a: 14.9 b: 45.8 c: 9.54 d: 7.47

vi). The separation or cut size of the hydrocyclone was (μm):

a: 2.0 b: 6.0 c: 9.4 d: 12

vii). The particle Reynolds number at the LZVV was:

a: 0.074 b: 0.12 c: 0.15 d: 0.30

9. Reitema's residence time model for an optimum design is given left, where L is total length. Using your answer for (8.vi) for the separation size, the hydrocyclone pressure drop was (bar):

a: 0.84 b: 3.4 c: 5.8 d: 7.9